Available online at www.sciencedirect.com
ScienceDirect
Journal of the European Ceramic Society 28 (2008) 1397–1403
www.elsevier.com/locate/jeurceramsoc

Integrating functional ceramics into microsystems

R.A. Dorey *,[a], S.A. Rocks, F. Dauchy, D. Wang, F. Bortolani, E. Hugo

Microsystems and Nanotechnology Centre, Building 70, Materials Department, Cranfield University, Cranfield, Bedfordshire MK43 0AL, UK

Available online 24 January 2008

Abstract

Micro electromechanical systems (MEMS) have applications in a diverse range of fields. The presence of a diverse range of materials imposes constraints in the design of, and use of fabrication technologies for, MEMS. In addition, the need to structure these materials on the micro-scale introduces additional challenges which need to be overcome. These issues are of particular importance when ceramics need to be incorporated into MEMS. It is of interest to incorporate ceramics into MEMS due to the desire to utilise their functional properties including piezoelectricity, ferroelectricity and conductivity.

This paper will present a review of some potential solutions developed by the authors and found in literature, focussing on low-temperature processing of functional ceramics, selective chemical patterning, micro-moulding, and direct writing. The capabilities of different techniques are compared and the relative advantages of each explored.

Keywords: Films; Shaping; Sol–gel processes; PZT; Functional applications

1. Introduction

Functional ceramics, such as dielectric, piezoelectric, pyroelectric, ferroelectric and conducting materials, are of great technological interest due to their ability to interact with the surrounding environment to sense, act upon and generate power. However, to make effective use of these materials it is necessary to combine them with other materials, and to structure these materials, to create a functioning device that can be applied to do useful work. Furthermore, by decreasing the size of the resultant devices improvements in terms of sensitivity, efficiency and portability can be realised.[1,2] It is for these reasons that microsystems, or micro electromechanical systems (MEMS), are of technological interest.[3]

While many functional ceramic materials are of technological interest, this paper will focus on the processing of lead zirconate titanate (PZT) as it is one of the most used piezo/ferroelectric materials[4] and exhibits processing challenges that are common to most other functional ceramics. PZT is a solid solution of lead titanate and lead zirconate and represents a family of materials with a range of compositions.

PZT has applications in a range of devices including ultrasound transducers, actuators, and sensors.[3,5] Macro-scale devices of this type are typically manufactured using an assembly type approach, where the individual parts are assembled, by bonding operations, and shaped by mechanical techniques such as cutting, grinding and polishing. While this approach is suitable for macro devices, the level of difficulty increases as the size of the devices decrease. In addition, unless the thickness of the bonding is scaled in line with the device, reductions in device performance can occur due to the presence of large volumes of inactive material. By adopting an alternative processing route where structures are built up using a layer-by-layer approach, smaller structures can be produced and batch processing methods can be applied with multiple devices being fabricated in parallel on a single support wafer. The challenges with such micro-scale assembly techniques are the requirements to integrate and co-process multiple materials, as well as shape the structures at very small sizes. This approach poses a number of challenges due to the contrasting materials employed in typical MEMS devices.

For the purposes of this paper, a cantilever type structure can be considered as a fair representation of a typical MEMS device as it possesses many of the features found in other common

* Corresponding author. Tel.: +44 1234 750111; fax: +44 1234 751346.
E-mail address: r.a.dorey@cranfield.ac.uk (R.A. Dorey).
[a] Dr. Dorey is a Royal Academy of Engineering/EPSRC research fellow.

0955-2219/$ – see front matter © 2007 Elsevier Ltd. All rights reserved.
doi:10.1016/j.jeurceramsoc.2007.12.003

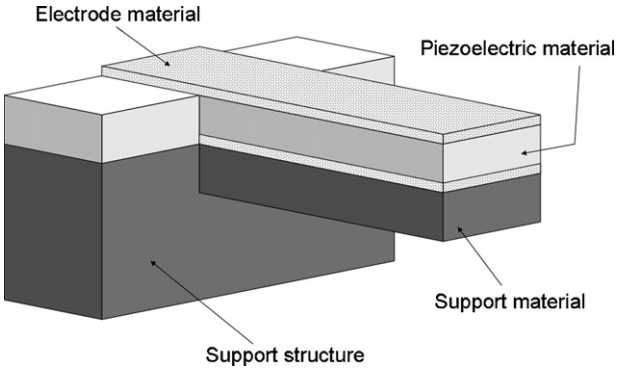

Fig. 1. Schematic of cantilever MEMS component showing key features common to many MEMS devices.

MEMS devices, such as diaphragms and bridges. Between them, these three types of MEMS structure can be used in a wide range of devices ranging from actuators and force sensors through to gas sensors and solid oxide fuel cells.

A cantilever device (Fig. 1) consists of a laminated composite beam comprising the support material and piezoelectric material. In addition, there is a requirement for electrical connections to be made to the piezoelectric material to allow actuation and/or sensing. The composite beam will itself be attached to a support structure to allow handling and connection of the device to the control electronics. Each of the materials found in the system impose certain constraints: functional ceramic materials are typically brittle and require high temperature processing; electrode materials are typically metals and have good electrical conductivity, high thermal expansion coefficients and may be susceptible to oxidation/corrosion; support materials are usually passive with a reasonable stiffness and ability to be shaped. They can be metals, polymers, ceramics or semiconductors. Typical dimensions for MEMS cantilevers are in the order of 100–2000 μm long, 10–500 μm wide, and 1–50 μm thick. Focussing only on the production of the ceramic films, it can be seen from this relatively simple structure that there are already a multitude of material processing challenges that need to be overcome if the ceramic is to be successfully integrated. A review of processing of functional ceramics for MEMS applications gives an overview of some techniques available to address these challenges.[5]

While achieving ceramic films 50 μm thick by machining is possible, there is a significant amount of material wastage and great care has to be taken to ensure uniformity and flatness if bonding and wafer level processing are to be successfully undertaken. For this reason, the most common routes for fabricating MEMS devices on this scale are layer-by-layer approaches where successive layers are deposited to build up the structure. The challenge with this approach is that the functional ceramic layer will typically require a high temperature processing stage for densification/consolidation.[5,6] For PZT the standard sintering temperature is in the region of 1200–1400 °C. At such temperatures materials such as metals, glasses, silicon and polymers would melt, vaporise or degrade. Even processing the functional ceramic at such temperatures can pose a problem. While 1200–1400 °C is used to sinter bulk PZT, it is usual to conduct the sintering in a lead-rich environment to counteract the lead loss due to evaporation. Even with this precaution it is very difficult to control the stoichiometry of the PZT near the surface of the material. As the size of the PZT component decreases in size, this surface zone becomes a greater proportion of the material resulting in a greater difficulty in controlling the composition. Hence, at the size scales required for a MEMS device, the use of a temperature of 1200–1400 °C is also undesirable from the point of view of processing the PZT.

The first step in integrating functional ceramics into microsystems is to reduce the temperature at which the ceramic is processed. Sintering aids and glass frits are commonly added to ceramic powders to reduce the temperature required to sinter ceramic materials. Using this approach, the sintering temperature can be reduced considerably and the use of sintering temperatures of 750–950 °C have been reported. Examples of sintering aids used for lead based piezoelectric materials include PbO,[7–10] PbO–Cu_2O,[11–13] $Pb_5Ge_3O_{11}$,[14–16] $LiBiO_2$–CuO,[17] PbO–PbF_2,[18] Bi_2O_3–B_2O_3–CdO,[18–20] borosilicate glass,[19,21,22] Li/PbO[23] and PbO/TiO_2.[24] The disadvantage of using glass frits and, to a lesser extent, sintering aids is that a second phase is introduced which can have a detrimental effect on the functional properties of the ceramic.

An alternative approach to using a powder route, with or without sintering aids or glass frit, is to employ a low-temperature ceramic deposition route. Physical vapour, chemical vapour and chemical solution deposition routes all allow ceramic films to be deposited at temperatures below 650 °C. Each route has relative advantages and disadvantages, yet for producing MEMS devices with ceramic components in the size range of 1–50 μm a chemical solution deposition (CSD) route is favoured as it is well suited to producing films over large areas, can offer very good compositional range and control, is able to produce a range of film thicknesses and is relatively simple and economic to use. To further increase the range of thicknesses achievable, a modified CSD can be employed. This paper presents work on this modified CSD route for the fabrication of thick ceramic films for integration into MEMS. By combining the low-temperature CSD sol–gel process with powder processing and sintering aids, ceramic films with densities in the region of 80–95% theoretical density can be produced at temperatures between 600 and 720 °C.[11,25] It is possible to use such low-sintering temperatures as the green density and sintering kinetics of the film are increased considerably by the presence of the sol–gel material. The addition of the small amount of sintering aid is then sufficient to further increase the density of the film by 5–10%. Using this route, functional ceramics have been incorporated with metals, silicon and glass to create a range of MEMS devices. Fig. 2 shows a 10 μm thick PZT film incorporated onto a glass substrate coated with a multilayer light emitting structure consisting of Mn-doped ZnS, $BaTiO_3$ and In-doped SnO on glass. The maximum processing temperature employed was 650 °C which prevented the Mn:ZnS from degrading during processing.[26] Despite the low-sintering temperature, the PZT exhibited a relative permittivity of 800 (70% of that of conventionally produced PZT of comparable composition).

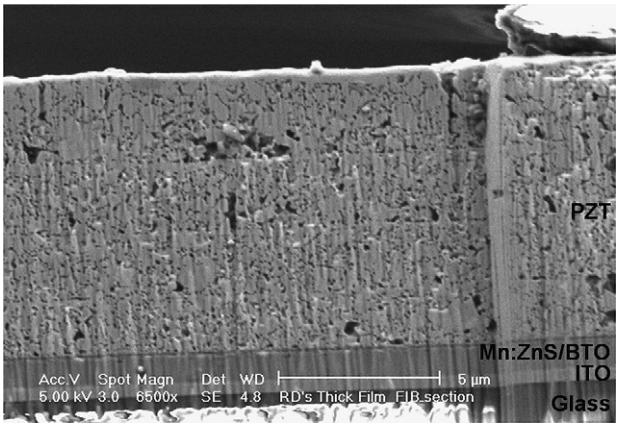

Fig. 2. PZT thick film incorporated onto a glass substrate with a ITO/BTO/Mn:ZnS interfacial layer.

2. Thick-film deposition

The modified CSD, or composite sol–gel, route involves creating a composite ink consisting of a ceramic powder, ceramic producing sol, sintering aids (if required) and dispersant. By varying the relative proportions of powder and sol it is possible to control the characteristics of the ink so that it can be used in different ways. A very low powder load is used for droplet deposition,[27,28] mid level powder loaded inks can be painted or spun onto substrates,[11] while high powder loaded inks can be screen printed.[29] By matching the composition of the sol to that of the powder, homogenous films can be produced. Alternatively, a sol with a different composition can be used to create a two material composite film.[30] Fig. 3 shows an example of a homogenous microstructure that can be achieved using the composite sol–gel approach in combination with sol infiltration and low-melting point sintering aid. Fig. 4 demonstrates the flexibility of the process showing how a TiN powder was used in conjunction with an Al_2O_3 sol to create an electrically conducting ceramic thick film.

While the use of the composite sol–gel route significantly reduces the temperature required to densify the functional ceramic material, reactions can still occur between two phases within the system. The risk of this occurrence is exasperated when atomic diffusion is accelerated through the addition of a liquid phase sintering aid. By utilizing a diffusion barrier layer such reactions can be minimised. For the case of PZT, where the Pb is known to react with Si, a 40 nm thick ZrO_2 diffusion barrier layer was found to be sufficient to prevent such reactions. The homogenous PZT film shown in Fig. 3 has such a ZrO_2 diffusion barrier in place and no evidence of this interfacial reaction is evident. This can be contrasted with Fig. 5, showing the effect when this diffusion barrier is not in place. While thicker diffusion barrier layers can also be used,[5] the advantage of using such a thin diffusion barrier layer is that its presence will not unduly affect the performance of the final MEMS device.

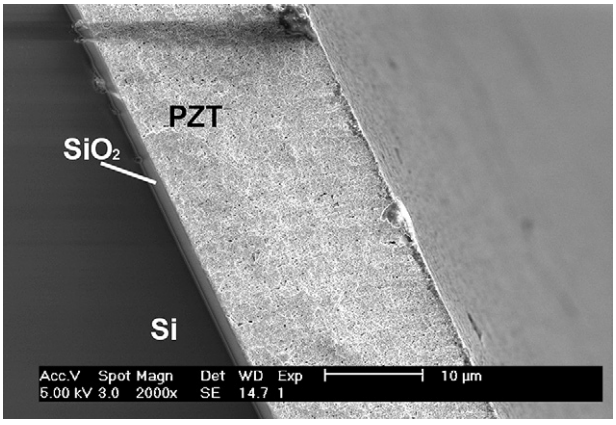

Fig. 3. Fracture cross-section of PZT thick film on a silicon substrate.

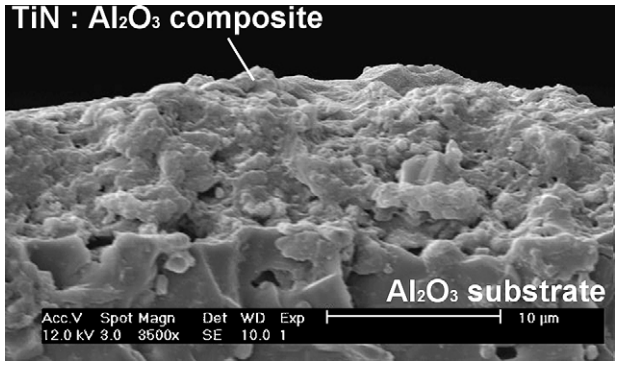

Fig. 4. Fracture cross-section of TiN/Al_2O_3 composite film on an Al_2O_3 substrate.

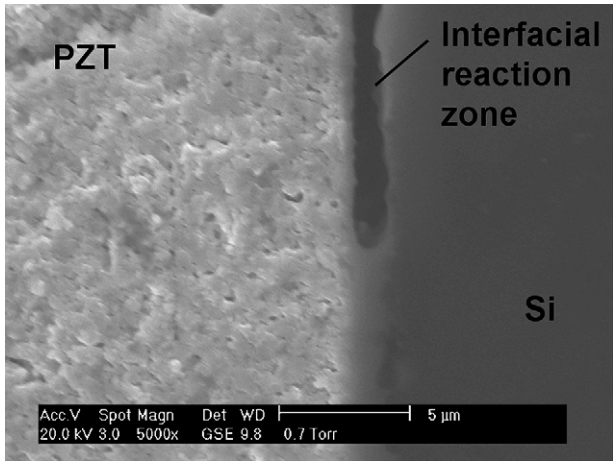

Fig. 5. Interfacial reaction zone produced as a result of reactions between the PZT and Si at 710 °C in the absence of an effective diffusion barrier layer.

3. Structuring of films

The successful incorporation of a functional ceramic with the electrode and substrate materials clearly demonstrates that MEMS devices utilising functional ceramics can potentially be realised. However, to produce a functional MEMS device, it is also necessary to shape the ceramic material. Such shaping can either be accomplished using a subtractive or an additive process route.

In subtractive patterning selected areas are protected using a masking material and then selectively attacked using chemical

and/or mechanical routes. In these processes it is first necessary to deposit a continuous film of the required thickness prior to the etching process.

In additive patterning ceramic material is placed where it is required. Perhaps the most recognised form of additive processing is ink jet printing which has successfully been used to produce macro scale ceramic structures.[31] The challenge with using such techniques for producing micro-scale devices is the difficulty in producing sufficiently fine droplets and accurately controlling the location of where these droplets are deposited.

4. Subtractive patterning

By far the most common route of subtractive structuring of PZT films for MEMS is that of chemical wet etching. For this work continuous thick films of PZT were deposited using a spin coating technique. Full details of the fabrication process are detailed in a previous publication.[11] Briefly, the sol used was based on a 2-methoxyethanol route. Starting reagents were lead acetate, zirconium isopropoxide, titanium propoxide, acetic acid and 2-methoxyethanol. The PZT powder–sol ink was composed of PZT powder (PZ26, Ferroperm, Denmark), PZT sol (1.1 M), sintering aid ($0.2Cu_2O/0.8PbO$) and dispersant (KR55, Kenrich petrochemical) in the proportions 1.5 g:1 ml:0.075 g:0.03 g. The films were deposited by coating the substrate with the ink and spinning the wafer at 2000 rpm for 30 s to produce a uniform film approximately 2.5 μm thick. The film was then dried at 200 °C and pyrolysed at 450 °C to convert the sol–gel phase to an amorphous oxide ceramic. A further layer was then deposited, again drying and pyrolysing the film, to increase the thickness to approximately 5 μm. The density of the composite layer was then increased by infiltrating the layer with pure sol (0.55 M) which was again spun at 2000 rpm, dried at 200 °C and pyrolysed at 450 °C. This process was repeated 4, 5 or 6 times to optimise the density of the film. This layering and infiltration process was then repeated until the required film thickness had been achieved. A cross-section of the resultant 22 μm thick film, composed of six 2 composite plus 4 infiltration layers, is shown in Fig. 3.

Selective areas of the PZT film were protected using a 5 μm thick layer of AZ4562 (Clariant, UK) photoresist material which was deposited by coating the sample with the liquid photoresist and spinning at 1000 rpm for 1 min followed by drying at 90 °C for 3 min. The photoresist was selectively exposed to UV light using a chromium-coated glass mask and developed in AZ351B (Clariant, UK). The wafer was then immersed in an aqueous solution of HF (0.5 vol%) and HCl (0.45 vol%) at 45 °C for 10 min to remove the exposed regions of PZT. A two-component etching solution is used due to the complex nature of the PZT. The HCl is used to etch the PbO and TiO_2 components while the ZrO_2 component is attacked by the HF. Due to the isotropic nature of the etching process, this process results in a characteristic side wall profile caused by the PZT material being etched laterally at the same rate that it is etched in the through thickness direction. In an ideal process this would result in a side wall angle of 45°. However, due to film porosity, slight anisotropy in etching rates and attack of the mask–PZT interface, this side wall angle is typically between 35 and 45°. Fig. 6 shows a confocal microscope image of an etched wall highlighting this side wall angle, the slight over-etching near the surface and slight under-etching near the substrate. This characteristic side wall angle limits the resolution of this etching process as the smallest spacing between two features will be directly related to the thickness of the film being etched. A separation of three times the thickness is typically achievable using the wet etching route. In addition to being thickness dependent, the resolution achievable is also time dependent as the etching process will continue as long as the etching solution is in contact with the ceramic. Once the entire thickness of the PZT has been removed to expose the substrate, the resolution will continue to degrade as lateral etching continues to take place. It is therefore important to monitor the progression of the etching process carefully. It should be remembered that this resolution is related to the separation of the top of the features and not the base of the features which, for the case of the best resolution, will barely be separated.

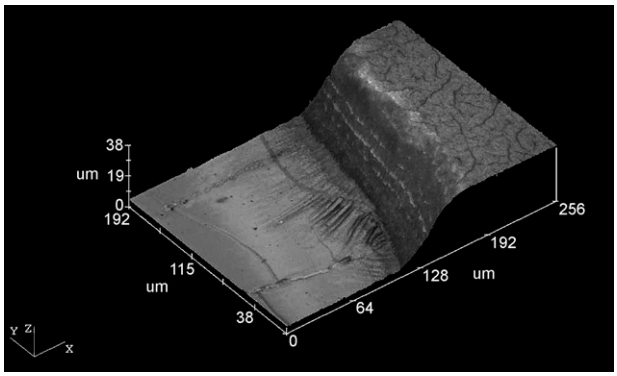

Fig. 6. Confocal microscope image of the edge of a wet-etched PZT feature on a silicon substrate.

For the etching of other functional ceramics, alternative etch chemistries may be used, but will still typically contain HF, HCl or HNO_3 due to the chemical nature of ceramics. However, comparable etch profiles are still observed as the etching process will not have been changed. During the PZT etching process, PbClF is produced as a reaction product and remains as a white precipitate which slows the etching process.[32,33] For thin film processing this PbClF is removed using a HNO_3 wash at the end of the etching process. As the thick film etching process takes longer to complete, the build up of PbClF can lead to a reduction in the etching rate. Unfortunately, it is not possible to remove this precipitate at regular intervals as the HNO_3 wash also removes the protective photoresist material. For this reason, a final HNO_3 wash is used for thick films and the reduction in etch rate needs to be accounted for when calculating etching times.

Mechanical etching can also be conducted using a similar process whereby a continuous film is selectively protected using an elastic material. Etching is then achieved by abrading the surface with high velocity powder particles. As with particle erosion, elastic materials exhibit significantly reduced etch (erosion) rates relative to those of brittle ceramics. For such mechanical etching, photoresist materials are again typically employed. Instead of chemical resistance, the photoresists are selected for their abrasion resistance and are typically elastomeric or metal-

lic in nature.[34] One feature of this etch process is that selectivity is achieved via mechanical properties and not chemical properties, as is the case in wet etching. Hence, while wet etching can be used to etch only the PZT material and leave the silicon substrate relatively undamaged, mechanical etching shows very little selectivity between the silicon and PZT. The side wall angles achievable with power blasting are considerably higher than those observed with chemical etching as the lateral etch rate is minimal due to the directed nature of the particle impacts. Despite this, high resolution is difficult to achieve as the separation of features needs to be larger than the diameter of the eroding particles, which are typically 10–50 μm in diameter. Finer separation can be achieved at the expense of the etch rate as the smaller particles have correspondingly lower momentums and etching capability. In addition, the use of finer particles raises additional concerns relating to the containment and capture of fine airborne particles.

Reactive ion etching and deep reactive ion etching use a combination of chemical and mechanical etching where ion bombardment is used to remove material on an atomic level using a chemo-mechanical action. These techniques have typically only been used to etch relatively thin pieces of ceramic due to the slower etch rates and greater cost of processing equipment. Again, continuous films are patterned by using a mask material that is etched at a slower rate than the ceramic film. Typically polymer masks can again be used.

5. Additive patterning

The alternative approach to fabricating ceramic features is a bottom up, or additive, process. Two such routes can be envisaged. The first involves placement of individual building blocks to create the desired structure. The second involves creating a mould and then creating a feature by filling and then removing this mould.

The direct placement approach used the placement of individual droplets of a ceramic ink to create the required structure. The challenge with using such a technique for producing features for MEMS is the required scale of the features. Droplets as small as a few tens of micrometers can routinely be created using ink jet printing[35,36] and electrohydrodynamic printing[37] techniques. When these droplets are deposited onto a surface they will produce relics that are 2–10 times the diameter of the droplets.[35] It is therefore relatively easy to produce individual droplets that have diameters a few tens of micrometers, as can be seen in the inset in Fig. 7. However, these droplets are of comparable size to the features that are of interest, meaning that the original analogy of building a wall through the combination of individual bricks is not currently strictly true for direct writing at this scale. The future challenges will be to develop techniques that are capable of forming and controlling droplets that are one or two orders of magnitude smaller than the current droplets. For practical applications, where feature sizes of a 50 μm are required, this would necessitate the creation and control of droplets 500 nm in diameter—comparable to the size of the current individual powder particles. Despite the current size limitations, it is still

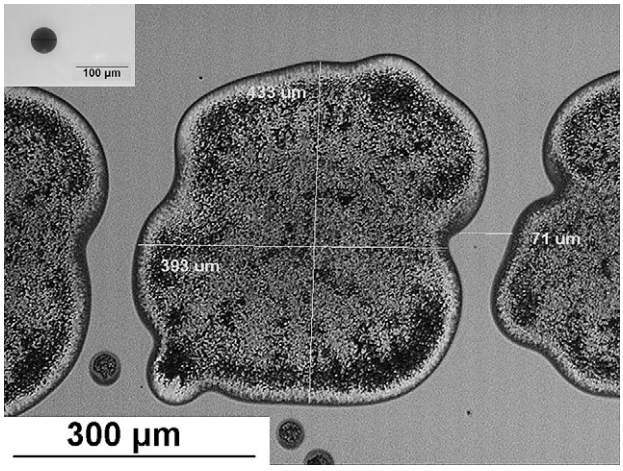

Fig. 7. Optical microscope image of a composite sol–gel feature on silicon deposited using inkjet printing (powder loading of ink was 0.083 g/ml of sol). Inset shows a single drop of coloured carrier fluid showing the print capabilities of an ink jet printer.

of interest to look at droplet-based deposition technologies for the creation of MEMS devices due to the great flexibility of the technologies. Using the composite sol–gel approach features of a few hundreds of micrometers have been created on silicon as can be seen in Fig. 7. Due to the individual droplet size and spreading of the droplet on the silicon surface it is difficult to control the precise shape of the feature. However, it does demonstrate that the composite sol–gel approach can successfully be used to create a feature with the PZT particles embedded in a sol–gel-derived matrix. Due to the low powder loading required to form an ink suitable for ink jet printing (0.083 g PZT powder/ml of sol, compared to the 1.5 g of PZT powder/ml of sol used for spin coating), the resultant microstructure, shown in Fig. 8, is different to that obtained using the spin coating route. For future applications, the powder-based inks is unlikely to yield sufficiently small droplets due to the size of the powder particles. Instead new inks containing nanoparticles can be used to create smaller droplets.[37]

The micro-moulding approach does not rely on the formation and control of small particles. Instead the shape of the

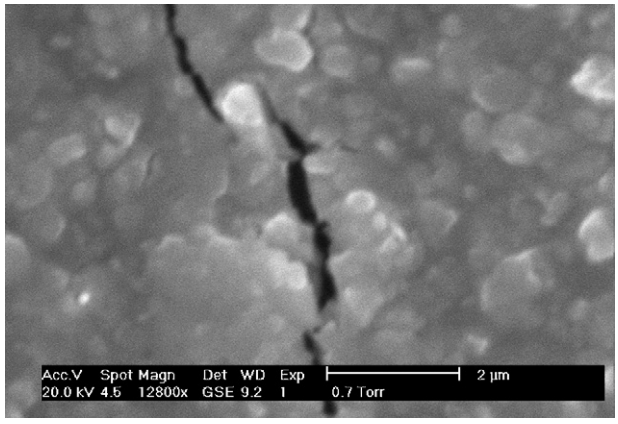

Fig. 8. SEM micrograph of PZT composite sol–gel feature produced using inkjet printing showing the PZT particles embedded in a sol–gel-derived matrix material.

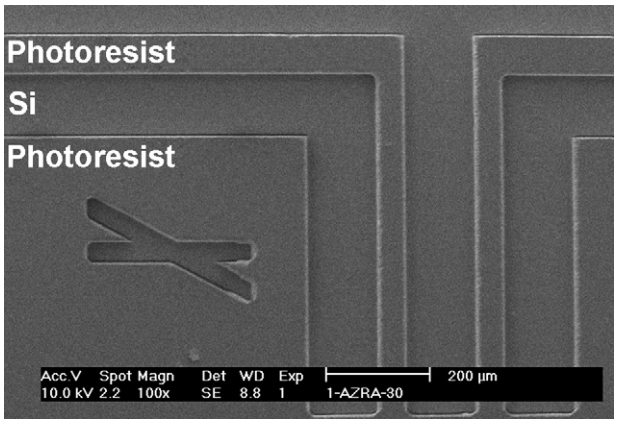

Fig. 9. Example of photoresist micro-mould in silicon.

features are dictated by the ability to shape the mould and control the shrinkage of the PZT during processing. The main requirements for the mould material are that it should be relatively easy to create and remove the moulds. For these reasons photoresist materials are again an attractive choice as the technology is readily available and known. In addition, the composite sol–gel-processing route can be modified to limit the maximum temperature, used during forming, to allow co-processing of the ceramic and polymeric materials. The composite sol–gel process is also a relatively low shrinkage process and so should allow good reproduction of the mould shapes.

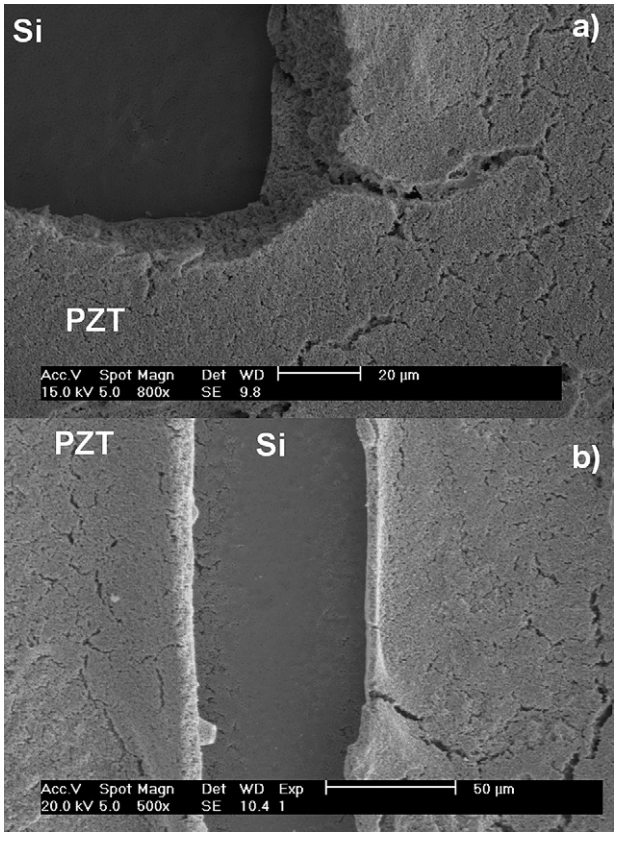

Fig. 10. Edges of PZT features produced using micro-moulding technique. (a) PZT aqueous slurry and (b) diol-based sol PZT slurry.

Moulds were created using thick photoresist selectively exposed to UV light (Fig. 9). The moulds were filled by spin coating either a powder slurry or composite sol–gel slurry onto the wafer containing the micro-moulds. Each individual layer was dried at temperatures below 200 °C to remove the carrier fluids and solvents and partially decompose the sol–gel materials. At temperatures below 200 °C the photoresist material is stable and does not undergo any structural or dimensional changes which may affect the moulding process. Subsequent infiltration and drying processes were then used to increase the green density of the feature prior to removal of the photoresist and sintering. The photoresist can either be removed during the sintering process or prior to it using an acetone wash. A range of different photoresist materials and composite sol–gel compositions have been studied.[38] The photoresists that are easier to remove are generally also attacked by the solvents found in the sol requiring either a modification in the sol chemistry or the use of a more resilient photoresist. Unfortunately, the photoresists that are more stable to chemical attack are also more difficult to remove at the end of the moulding process. Fig. 10 shows the edges of features produced using the micro-moulding process. Both a composite sol–gel ink (b) and an aqueous suspension of powder later infiltrated with sol (a) were used to create the features. In both cases the side wall angle and edge quality are much improved in comparison to the features produced using the wet etching route.

6. Conclusions

No single processing route is suited to produce all micro-scale features for use in MEMS. Instead they should be considered as a suite of techniques that, together, can be used to integrate and shape functional ceramics for use as MEMS devices. The relative suitability of the different techniques can be examined by considering the capabilities of each technique in terms of achievable minimum feature size, resolution and accuracy, with reference to the requirements for the final device.

The minimum feature size achievable using the wet deposition process is limited by the size of the individual droplets and the ability to control their deposition. Typically this will limit the minimum size to above 50 μm with a limit in the complexity of said shapes due to the need to combine individual droplets. Smaller features can be achieved using the subtractive etching and additive moulding routes. As the shapes are controlled by the mask/mould material shaping process, a greater range of shapes can be realised as this is controlled by the ability to shape the photolithographic materials. The minimum feature size will increase as the thickness increases where isotropic etching routes are employed.

In a similar manner, the maximum resolutions of the processes are limited by the ability to shape the ceramic as the resolution of mask/mould process is much greater. The moulding techniques should yield the highest resolution as it is the mould material that will define the separation between two features. With the subtractive processing routes the resolution will be limited by the isotropic etching size of mechanical abrasive used. The possible exception is if reactive ion etching techniques

are used where an anisotropic etch could be achieved. The resolution achievable using the droplet deposition would be limited by the size of the drops and the spreading of the droplets on the surface.

Accuracy of the processing using photolithography is defined by the accuracy of the photolithographic mask used to create the structures. Wet etching will have an additional constraint due to the lateral etching which will influence the size of the features, but not their relative position, if over-etching occurs. Droplet-based technologies will be limited by the ability to accurately control the location of the droplets and also their spreading once they hit the substrate.

In terms of application, the absence of a mask, and the economic and time cost associated with its manufacture, make the droplet-based process very attractive for prototyping, small runs with larger features. For larger runs where etching is not critical, then wet etching will probably continue to dominate due to the existing levels of know-how. Moulding will find application in niche applications where high resolution, small features are required. In all cases the inks used will dictate the ultimate thickness, sizes and resolutions of features.

References

1. Jeon, Y., Seo, Y. G., Kim, S.-J. and No, K., Low temperature sintering of screen-printed $Pb(ZrTi)O_3$ thick films. *Integr. Ferroelectr.*, 2000, **30**, 91–101.
2. Simon, L., Le Dren, S. and Gonard, P., PZT and PT screen-printed thick films. *J. Eur. Ceram. Soc.*, 2001, **21**, 1441–1444.
3. Setter, N., *J. Eur. Ceram. Soc.*, 2001, **21**, 1279–1293.
4. Koch, M., Evans, A. and Bunnschweiler, *Microfluidic Technology and Applications*. Research Studies Press Ltd., Baldock, Hertfordshire, England, 2000, p. 137.
5. Dorey, R. A. and Whatmore, R. W., Electroceramic thick film fabrication for MEMS. *J. Electroceram.*, 2004, **12**, 19–32.
6. Spearing, S. M., Materials issues in microelectromechanical systems (MEMS). *Acta Mater.*, 2000, **48**, 179–196.
7. Futakuchi, T., Nakano, K. and Adachi, M., Low-temperature preparation of lead-based ferroelectric thick films by screen printing. *Jpn. J. Appl. Phys.*, 2000, **39**, 5548–5551.
8. Farrari, V., Marioli, D., Taroni, A. and Ranucci, E., Multisensor array of mass microbalances for chemical detection based on resonant piezo-layers of screen-printed PZT. *Sens. Actuators B*, 2000, **68**, 81–87.
9. De Cicco, G., Morton, B., Dalmonego, D. and Prudenziati, M., Pyroelectricity of PZT-based thick films. *Sens. Actuators*, 1999, **76**, 409–415.
10. Prudenziati, M., Morten, B. and De Cicco, G., Piezoelectric thick-film materials and sensors. *Microelectron. Int.*, 1995, **38**, 5–11.
11. Dorey, R. A., Stringfellow, S. B. and Whatmore, R. W., Effect of sintering aid and repeated sot infiltrations on the dielectric and piezoelectric properties of a PZT composite thick film. *J. Eur. Ceram. Soc.*, 2002, **22**, 2921–2926.
12. Corker, D. L., Whatmore, R. W., Ringgaard, E. and Wolney, W. W., Liquid phase sintering of PZT ceramics. *J. Eur. Ceram. Soc.*, 2000, **20**, 2039–2045.
13. Corker, D. L., Zhang, Q., Whatmore, R. W. and Perrin, C., PZT 'composite' ferroelectric thick films. *J. Eur. Ceram. Soc.*, 2002, **22**, 383–390.
14. Tran-Huu-Hue, P., Levassort, F., Meulen, F. V., Holc, J., Kosec, M. and Lethiecq, M., Preparation and electromechanical properties of PZT/PGO thick films on alumina substrate. *J. Eur. Ceram. Soc.*, 2001, **21**, 1445–1449.
15. Hayashi, T., Inoue, T. and Akiyama, Y., Low temperature sintering of PZT powders coated with $Pb_5Ge_3O_{11}$ by sol–gel method. *J. Eur. Ceram. Soc.*, 1999, **19**, 999–1002.
16. Duval, F. F. C., Dorey, R. A., Zhang, Q. and Whatmore, R. W., Lead germanium oxide sinter-assisted PZT composite thick films. *J. Eur. Ceram. Soc.*, 2003, **23**(11), 1935–1941.
17. Wang, X. X., Murakami, K., Sugiyama, O. and Kaneko, S., Piezoelectric properties, densification behaviour and microstructural evolution of low temperature sintered PZT ceramics with sintering aids. *J. Eur. Ceram. Soc.*, 2001, **21**, 1367–1370.
18. Le Dren, S., Simon, L., Gonnard, P., Troccaz, M. and Nicolas, A., Investigation of factors affecting the preparation of PZT thick films. *Mater. Res. Bull.*, 2000, **35**, 2037–2045.
19. Thiele, E. S. and Setter, N., Lead zirconate titanate particle dispersion in thick-film ink formulations. *J. Am. Ceram. Soc.*, 2000, **83**, 1407–1412.
20. Wang, M.-C., Huang, M.-S. and Wu, N.-C., Effects of $30B_2O_3$–$25Bi_2O_3$–45CdO glass addition on the sintering of $12Pb(Ni_{1/3}Sb_{2/3})O_3$–$40PbZrO_3$–$48PbTiO_3$ piezoelectric ceramics. *J. Eur. Ceram. Soc.*, 2001, **21**, 695–700.
21. Beeby, S. P., Blackburn, A. and White, N. M., Processing of PZT piezoelectric thick films on silicon for microelectromechanical systems. *J. Micromech. Microeng.*, 1999, **9**, 218–229.
22. Maas, R., Koch, M., Harris, N. R., White, N. M. and Evans, A. G. R., Thick-film printing of PZT onto silicon. *Mater. Lett.*, 1997, **31**, 109–112.
23. Van Tassel, J. and Randall, C. A., Electrophoretic deposition and sintering of thin/thick PZT films. *J. Eur. Ceram. Soc.*, 1999, **19**, 955–958.
24. Prudenziati, M., *Thick Film Sensors*. Elsevier, NL, 1994, ISBN 0444897232, pp. 113–124.
25. Barrow, D. A., Petroff, T. E., Tandon, R. P. and Sayer, M., Characterisation of thick lead zirconate titanate films fabricated using a new sol–gel based process. *J. Appl. Phys.*, 1997, **81**(2), 876–881.
26. Munasinghe, C., Heikenfeld, J., Dorey, R., Whatmore, R., Bender, J. P., Wager, J. F. and Steckl, A. J., High brightness ZnS and GaN electroluminescent devices using PZT thick dielectric layers. *IEEE Trans. Electron Dev.*, 2005, **52**, 194–203.
27. Olding, T., Sayer, M. and Barrow, D., Ceramic sol–gel composite coatings for electrical insulation. *Thin Solid Films*, 2001, **398–399**, 581–586.
28. Kobayashi, M., Golding, T. R., Sayer, M. and Jen, C.-K., Piezoelectric thick film ultrasonic transducers fabricated by a sol–gel spray technique. *Ultrasonics*, 2002, **39**, 675–680.
29. Dorey, R. A., Whatmore, R. W., Beeby, S. P., Torah, R. N. and White, N. M., Screen printed PZT composite thick films. *Integr. Ferroelectr.*, 2004, **63**, 601–604.
30. Dorey, R. A. and Whatmore, R. W., Pyroelectric properties of PZT/PMNZTU composite thick films. *J. Elecroceram.*, 2004, **12**(3), 191–196.
31. Morissette, S. L., Lewis, J. A., Clem, P. G., Cesarano III, J. and Dimos, D. B., Direct-write fabrication of $Pb(Nb,Zr,Ti)O_3$ devices: influence of paste rheology on print morphology and component properties. *J. Am. Ceram. Soc.*, 2001, **84**(11), 2462–2468.
32. Zheng, K., Lu, J. and Chu, J., Study on wet-etching of PZT thin film. In *Microprocesses and Nanotechnology Conference International 2003 Digest of Papers, Vols. 29–31*, 2003, pp. 248–249.
33. Dauchy, F. and Dorey, R. A., Patterned crack-free PZT thick films for microelectromechanical system applications. *Int. J. Adv. Manuf. Technol.*, 2007, **33**(1–2), 86–94.
34. Wilson, S. A., Haigh, R. D., Southin, J. E. A., Dorey, R. A. and Whatmore, R. W., Design of spiral piezoelectric cantilever unimorphs for microactuation. In *Proceedings of the Euspen Congress*, 2003.
35. Lewis, J. A., Direct-write assembly of ceramics from colloidal inks. *Curr. Opin. Solid State Mater. Sci.*, 2002, **6**, 245–250.
36. Park, J., Moon, J., Shin, H., Wang, D. and Park, M., Direct-write fabrication of colloidal photonic crystal microarrays by ink-jet printing. *J. Colloid Interf. Sci.*, 2006, **298**, 713–719.
37. Rocks, S. A., Wang, D., Sun, D., Jayasinghe, S. N., Edirisinghe, M. and Dorey, R. A., Direct writing of lead zirconate titanate piezoelectric structures by electrohydrodynamic atomisation. *J. Electroceram.*, 2007, **19**, 287–293.
38. Navarro, N., Rocks, S. A. and Dorey, R. A., Micromoulding of lead zirconate titanate (PZT) structures for MEMS. *J. Electroceram.*, 2007, **19**, 321–326.